

Virtual Compton Scattering

H. FONVIEILLE

for the Jefferson Lab Hall A and VCS Collaborations

*Laboratoire de Physique Corpusculaire IN2P3-CNRS
Université Blaise Pascal Clermont-II, F63177 Aubière Cedex, France*

Abstract

Virtual Compton Scattering off the proton: $\gamma^*p \rightarrow \gamma p$ is a new field of investigation of nucleon structure. Several dedicated experiments have been performed at low c.m. energy and various momentum transfers, yielding specific information on the proton. This talk reviews the concept of nucleon Generalized Polarizabilities and the present experimental status.

Virtual Compton Scattering (VCS) off the proton: $\gamma^*p \rightarrow \gamma p$ has emerged within the last ten years as a powerful tool to study the internal structure of the nucleon, bringing forward exciting new concepts and observables. The field can be subdivided according to different c.m. energy domains.

At high energy ($s \gg M_N^2$) and large momentum transfer ($Q^2 \gg M_N^2$), QCD factorization allows the use of the VCS process to access: i) the nucleon Generalized Parton Distributions (GPDs) via Deep VCS at small t [1] ; ii) the nucleon Distribution Amplitudes via hard Compton scattering at large t [2].

At low energy, the VCS process gives access to the nucleon Generalized Polarizabilities or GPs, which are the main focus of this talk. The basic concepts are introduced and an experimental review is given of the experiments performed in the threshold regime ($\sqrt{s} \leq (M_N + M_\pi)$) and resonance region.

1 Concept of Generalized Polarizabilities

These are the generalization to a non-zero Q^2 of the polarizabilities introduced in Real Compton Scattering (RCS).

Let us recall that polarizabilities measure how much the internal structure of a composite particle is deformed when an external EM field is applied. The description of

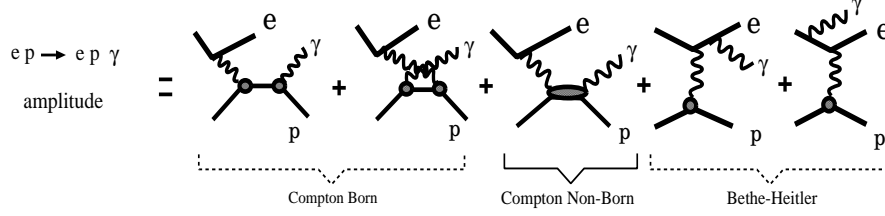


Figure 1: Decomposition of the photon electroproduction amplitude into: Born (s and u channels), Non-Born, and BH contributions.

the RCS process at low energy involves six polarizabilities (α, β , and $\gamma_i, i = 1, 2, 3, 4$) which parametrize the unknown part of nucleon structure, due to its internal EM deformation (see ref.3 and references therein). Performed since the sixties, RCS experiments have measured the proton electric and magnetic polarizabilities α_E and β_M [3], the results of which can be summarized as: i) the proton is a rather rigid object (polarizabilities are small), ii) β_M is smaller than α_E , due to a cancellation between its paramagnetic and diamagnetic contributions.

These observables can be generalized to any Q^2 , such that in VCS at low energy one probes the nucleon polarizability locally inside the particle, with a distance scale given by Q^2 . Equivalently, VCS can be seen as elastic scattering on a nucleon placed in an applied EM field, and hence the GPs can be seen as a measurement of “distorted” form factors. In all cases these observables are intrinsic characteristics of the particle, and provide a valuable and original test of models describing nucleon structure.

1.1 Photon electroproduction amplitude

VCS is accessed by photon electroproduction $ep \rightarrow ep\gamma$, which is the coherent sum of the Compton process and the Bethe-Heitler (BH) process, or electron bremsstrahlung; see Fig. 1. The main kinematic variables are defined in Fig. 2: the initial and final photon three-momenta q and q' and the final photon angles θ_{cm} and ϕ , in the (γp) center of mass. The $(ep \rightarrow ep\gamma)$ kinematics is fully defined by these four variables plus the virtual photon polarisation ϵ .

The low-energy behavior of the amplitude $T^{ee\gamma}$ has first been worked out by P. Guichon *et al* [4]. Only a brief summary is given here, and more details can be found in ref.5. The Compton amplitude decomposes into a Born term, characterized by a proton in the intermediate state, and a Non-Born term containing all other intermediate states. The BH and Born amplitudes are entirely calculable, with

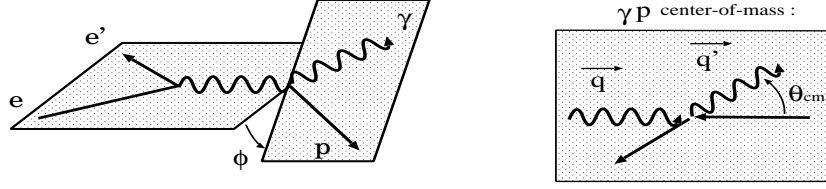


Figure 2: VCS kinematic variables.

Table 1: The six lowest order Generalized Polarizabilities (also called dipole GPs, due to $l' = 1$).

final γ	initial γ^*	S proton spin-flip	$P^{(\rho'l'\rho l)S}(q)$	$P^{X \rightarrow Y}$	$Q^2 = 0$ RCS limit
E1	C1	0	$P^{(01,01)0}$	$PC1 \rightarrow E1$	$\frac{-4\pi}{e^2} \sqrt{\frac{2}{3}} \alpha$
E1	C1	1	$P^{(01,01)1}$	$PC1 \rightarrow E1$	0
M1	M1	0	$P^{(11,11)0}$	$PM1 \rightarrow M1$	$\frac{-4\pi}{e^2} \sqrt{\frac{8}{3}} \beta$
M1	M1	1	$P^{(11,11)1}$	$PM1 \rightarrow M1$	0
E1	M2	1	$P^{(01,12)1}$	$PM2 \rightarrow E1$	$\frac{-4\pi}{e^2} \frac{\sqrt{2}}{3} \gamma_3$
M1	C2	1	$P^{(11,02)1}$	$PC2 \rightarrow M1$	$\frac{-4\pi}{e^2} \sqrt{\frac{8}{27}} (\gamma_2 + \gamma_4)$

proton EM form factors as inputs. The Non-Born amplitude T_{NB} contains the unknown part of the nucleon structure. Below pion threshold a Low Energy Theorem (LET) allows to expand T_{NB} in powers of q' ; the first term of the expansion is a known analytical function of six independent GPs, which are the goal of the measurements.

These GPs are derived from a multipole expansion of T_{NB} . One defines multipole amplitudes $H_{NB}^{(\rho'l'\rho l)S}$ according to the two involved EM transitions: ρ (ρ') stands for initial (final) photon polarization states (0, 1, 2 = longitudinal, magnetic, electric), l (l') is the total angular momentum of the initial (final) transition, and $S = (0), 1$ stands for proton (non)spin-flip. The H_{NB} multipoles depend on photon momenta q and q' . The GPs are defined (up to dimensional factors) as the limit of H_{NB} when $q' \rightarrow 0$, i.e. in the limit of a static EM field; they are denoted $P^{(\rho'l'\rho l)S}$ and depend only on q . Table 1 summarizes the notations for the two scalar ($S = 0$) and the four spin GPs ($S = 1$), and also shows their continuity to the real photon point ($Q^2 = 0$).

Below pion threshold, the VCS amplitude is purely real; above pion threshold it becomes complex, and resonances can be produced on-shell. One may say that the GPs are conceptually linked to the contribution of virtual resonant intermediate states, extrapolated down to $q' = 0$.

1.2 Photon electroproduction cross section

The photon electroproduction cross section is evaluated from the relation: $|T^{ee\gamma}|^2 = |T_{BH+Born}|^2 + 2\text{Re}(T_{BH+Born} \times T_{NB}) + |T_{NB}|^2$. Below pion threshold, $|T_{NB}|^2$ can be neglected and thus the GPs are extracted via the interference term (BH+Born)(NB). The LET leads to the following expression for the unpolarized cross section:¹

$$d\sigma(ep\gamma) = d\sigma_{BH+Born} + (P.S.) \times \left[v_1 \left(P_{LL}(q) - \frac{1}{\epsilon} P_{TT}(q) \right) + v_2 \left(P_{LT}(q) \right) \right] + O(q'^2), \quad (1)$$

where $(P.S.)$ is a phase space factor and v_1, v_2 are known kinematic coefficients [5]. The two structure functions $(P_{LL} - \frac{1}{\epsilon} P_{TT})$ and P_{LT} are linear combinations of the GPs, given e.g. by the following choice: [5]

$$\begin{aligned} P_{LL}(q) &= -2\sqrt{6} M_N G_E(\tilde{Q}^2) P^{(01,01)0}(q) \\ P_{TT}(q) &= -3 G_M(\tilde{Q}^2) \frac{q^2}{\tilde{q}_0} \times \left[P^{(11,11)1}(q) - \sqrt{2}\tilde{q}_0 P^{(01,12)1}(q) \right] \\ P_{LT}(q) &= \sqrt{\frac{3}{2}} \frac{M_N q}{\tilde{Q}} G_E(\tilde{Q}^2) P^{(11,11)0}(q) + \frac{3}{2} \frac{\tilde{Q} q}{\tilde{q}_0} G_M(\tilde{Q}^2) P^{(01,01)1}(q), \end{aligned}$$

where \tilde{Q}^2 , \tilde{q}_0 , \tilde{Q} are specific kinematic variables². So in an unpolarized experiment performed at fixed q and ϵ , one measures two structure functions: $(P_{LL} - \frac{1}{\epsilon} P_{TT})$ sensitive to the electric GP $\alpha(Q^2) \sim P^{(01,01)0}$, and P_{LT} sensitive to the magnetic GP $\beta(Q^2) \sim P^{(11,11)0}$.

1.3 Methods to extract GPs

Two methods are presently used to extract GPs from absolute $(ep\gamma)$ cross sections.

- **Method 1** is based on the LET, and only works below pion threshold. In bins of photon angles (θ_{cm}, ϕ) , one forms the quantity $(d\sigma_{exp} - d\sigma_{BH+Born})/(P.S.)$ measured at finite q' , and extrapolates it to $q' = 0$ to obtain the term in brackets in eq. 1. Present experimental data suggest that, at least in most of the phase space, the extrapolation can be done assuming that the $O(q'^2)$ contribution in eq. 1 is negligible. The bracketed term is then easily fitted as a linear combination of the two structure functions $(P_{LL} - \frac{1}{\epsilon} P_{TT})$ and P_{LT} at fixed q and ϵ .

- **Method 2** is based on the formalism of Dispersion Relations (DR) [6] and works below pion threshold as well as in the first resonance region. In this model the

¹ $d\sigma$ is a short notation for the fivefold differential cross section $d^5\sigma/d\Omega_{e'}^{lab} dk'^{lab} d\Omega_p^{cm}$.

² The important notion is that \tilde{Q}^2 is equivalent to q .

Table 2: VCS experiments.

experiment $ep \rightarrow ep\gamma$	Q^2 (GeV ²)	(γ^*p) c.m. energy \sqrt{s}	p cone $\theta_{pq \text{ lab}}$	data taking	status (@ end 2001)
MAMI A1	0.33	$< (M_N + M_\pi)$	10°	1995+97	published
JLab E93-050	1.0, 1.9	$< 1.9 \text{ GeV}$	$6^\circ, 3^\circ$	1998	final stage
Bates E97-03	0.05	$< (M_N + M_\pi)$	28° OOPS	2000	analysis
Bates E97-05	0.12	$\sim 1.232 \text{ GeV}$	$14\text{-}20^\circ$ OOPS	2001	analysis

imaginary part of the VCS amplitude is given by the sum of πN intermediate states, computed from $\gamma^*N \rightarrow \pi N$ data (MAID model), plus higher order contributions which are not constrained by the model. The latter have to be fitted to the VCS data, under the form of two free parameters Λ_α and Λ_β describing the Q^2 -dependence of the scalar GPs α and β . The knowledge of the parameters at a given value of Q^2 then yields the model prediction for the structure functions P_{LL} , P_{TT} and P_{LT} at this momentum transfer.

1.4 GP effect on cross sections

Figure 3-left shows the various components of the photon electroproduction cross section, in and out of the leptonic plane, for selected kinematics. The Bethe-Heitler peak is dominant around the incident and scattered electron directions; as one goes out-of-plane it fades away, giving a smoother cross section behavior. Figure 3-right shows the expected effect of GPs on the cross section, as given by two different calculations: the lowest order (or bracketed) term of eq. 1, and the full DR prediction. Out-of-plane, the GP effect is roughly constant, of the order of -10 %. In-plane the GP effect has a more complicated pattern, due to the BH interference.

2 Experiments

Table 2 summarizes the VCS experiments performed so far. All of them have detected the scattered electron and outgoing proton in high-resolution magnetic spectrometers, selecting the exclusive photon channel by the missing-mass technique. Also, being unpolarized experiments, they all measure the same two structure functions, at different values of q . An accurate determination of the absolute five-fold cross sections is necessary, due to the relatively small polarizability effect.

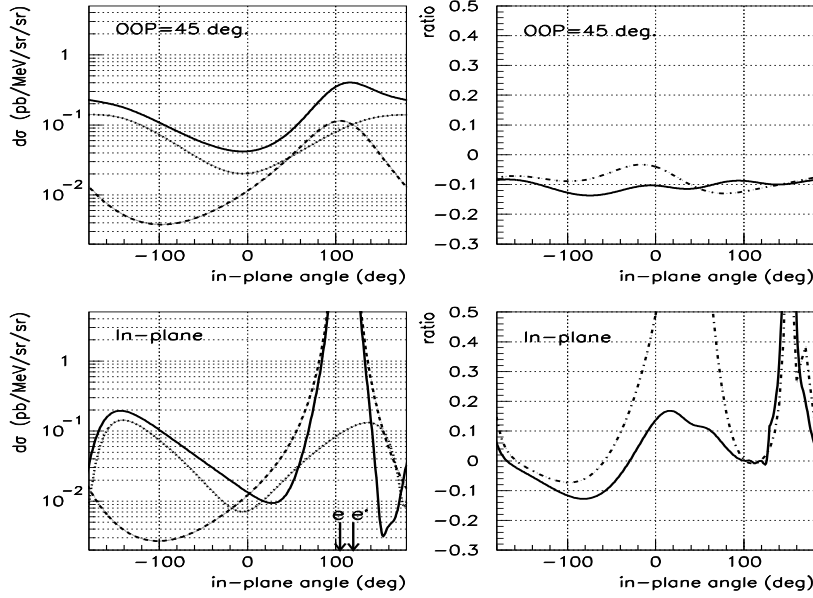


Figure 3: $(ep \rightarrow ep\gamma)$ cross section components for: $q = 1.08$ GeV/c, $q' = 105$ MeV/c, and $\epsilon = 0.95$. The abscissa is the azimuthal angle of the outgoing photon when the polar axis is chosen perpendicular to the leptonic plane. “OOP” is the polar angle using this convention. Left plots: BH+Born (solid), BH (dashed), and Born (dotted) contributions. Right plots: the ratio $(d\sigma_{GP} - d\sigma_{BH+Born})/d\sigma_{BH+Born}$ for two calculations of $d\sigma_{GP}$: i) a first order GP effect, taking $P_{LL} - \frac{1}{\epsilon}P_{TT} = 2.3$ GeV⁻² and $P_{LT} = -0.5$ GeV⁻² (solid), ii) a DR calculation for parameter values $\Lambda_\alpha = 0.92$ GeV, $\Lambda_\beta = 0.66$ GeV (dash-dotted).

2.1 The MAMI experiment

The Mainz experiment [7] measured photon electroproduction cross sections in the leptonic plane, at $Q^2 = 0.33$ GeV². The two structure functions $P_{LL} - P_{TT}/\epsilon$ and P_{LT} were determined using the LET method as described in section 1.3, at $q = 0.6$ GeV/c and $\epsilon = 0.62$. Results are plotted in Fig. 4; they show good agreement with the calculation of Heavy Baryon Chiral Perturbation Theory [8]. Several models predict an extremum of P_{LT} at low Q^2 , a feature which will be interesting to confirm experimentally. This turnover can be related to the behavior of the para- and diamagnetic contributions to the β polarizability. In CHPT it originates from the pion cloud, which yields a diamagnetic contribution of positive sign, visible at low Q^2 . For a review of model predictions see ref.9.

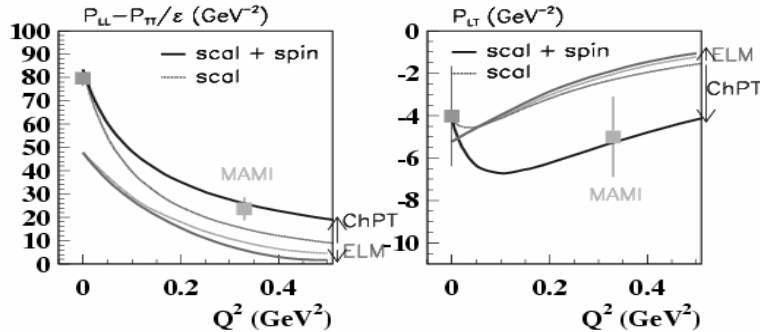


Figure 4: VCS unpolarized structure functions measured at Mainz [7] and their value at the real photon point [3]. The curves represent two model predictions (ChPT [8] and ELM [10]), including (in dark grey) or not including (in light grey) the spin GPs (effect indicated by an arrow).

2.2 The BATES experiments

The Bates experiment 97-03 [11] has been performed at $Q^2 = 0.05 \text{ GeV}^2$, i.e. in the region of the expected turnover of P_{LT} . Measurements have been done in-plane and at 90° out-of-plane, using the OOPS spectrometers. The experiment covers a limited range in polar angle θ_{cm} around 90° , so the structure functions will be extracted mostly from the ϕ -dependence of the cross section. Data analysis is in progress, presently concentrating on Monte-carlo studies and absolute normalization. This experiment represents a Lab achievement, having made the first use of the high duty factor beam in the South Hall Ring and of the full OOPS system. The Bates experiment 97-05 [12] has been performed at $Q^2 = 0.12 \text{ GeV}^2$ to study the $N \rightarrow \Delta$ transition, and data analysis is also in progress.

2.3 The JLab experiment

Experiment E93-050 [13] was performed in Hall A of the Thomas Jefferson National Accelerator Facility (JLab) at $Q^2 = 1.0$ and 1.9 GeV^2 . Data covers the region below pion threshold, and the resonance region up to $\sqrt{s} = 2 \text{ GeV}$ at $Q^2 = 1.0 \text{ GeV}^2$.

The strong Lorentz boost from γp center-of-mass to lab focuses the outgoing proton in a narrow cone (see Table 2) allowing the hadron arm acceptance to cover the full phase space of the outgoing photon in c.m. The key points to obtain accurate cross sections are a detailed Monte-carlo simulation (including radiative corrections) and a

detailed study of cuts in order to eliminate background, mainly due to punchthrough protons.

Absolute normalization is checked in two ways: i) by computing the ($ep \rightarrow ep$) cross section from elastic data taken during the experiment; ii) using the VCS data, namely the important property that the ($ep\gamma$) cross section should tend to the known (BH + Born) cross section when the final photon momentum q' tends to zero³. Both tests show that the absolute normalization is correct within 1-2 percent, when using the most recent determination of proton form factors: the JLab measurement of the ratio $\mu G_E/G_M$ [14] and the G_M fit of ref.15.

• **Analysis below pion threshold:** photon electroproduction cross sections have been obtained at fixed $q = 1.08(1.60)$ GeV/c and fixed $\epsilon = 0.95(0.88)$, corresponding to the data set at $Q^2 = 1.0$ (1.9) GeV². As an example, Fig. 5 shows some of the out-of-plane cross sections measured for both data sets. These data illustrate how the (small) GP effect increases with q' and how its shape agrees with the LET prediction. More details can be found in ref.17.

The quantity $(d\sigma_{exp} - d\sigma_{BH+Born})/(P.S.)$ of eq. 1 does not show any noticeable q' -dependence, so it is averaged over q' and then fitted according to the first method of section 1.3. The fit is performed on (in-plane + out-of-plane) cross sections and gives a reasonably good χ^2 , confirming the validity of the low-energy expansion at these rather high Q^2 . Numerical results are reported in Table 3. A second analysis of this data below pion threshold is presently underway, based on the DR model. A preliminary result at $Q^2 = 1.9$ GeV² is included in Table 3.

• **Analysis in the resonance region:** these are the first VCS measurements ever performed in this kinematic domain. The initial goal was to study how resonances couple to the doubly EM channel, and search for possible missing resonances. Doing an excitation scan in $W = \sqrt{s}$ from M_N to 1.9 GeV, cross sections have been determined at a fixed $Q^2 = 1.0$ GeV², backward angle $\theta_{cm} = 167.2^\circ$ and beam energy 4.032 GeV [16]. They are presented in Fig. 6 as a function of W for various azimuthal angles ϕ . The DR model reproduces well the Delta region. Using these data, the second method of section 1.3 has been applied for the first time. The free parameters of the DR model are adjusted by a χ^2 minimization, yielding the values of the two structure functions at $Q^2 = 1.0$ GeV² and $\epsilon = 0.95$. Results are reported in Table 3.

³indeed, in eq. 1 the bracketed term is of order $(q')^0$ and the phase space factor ($P.S.$) is of order $(q')^1$.

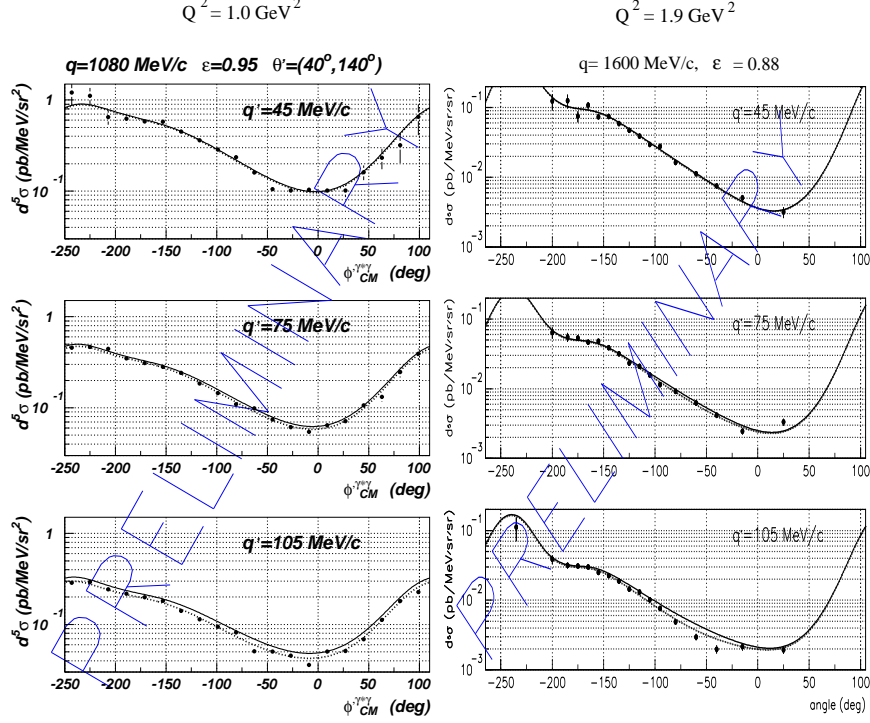


Figure 5: $(ep \rightarrow ep\gamma)$ cross sections measured at JLab versus in-plane angle, for OOP= 50° (left) and 25° (right). Error bars are statistical only. The angle in abscissa is the same as in Fig. 3. The curves correspond to: BH+Born calculation (solid) and a first order GP effect (dotted).

2.4 Results summary

Table 3 summarizes our present knowledge of the two structure functions measured in unpolarized VCS: the MAMI result, and the preliminary JLab results obtained so far, both below and above pion threshold. One first notices the fast decrease of the observables with Q^2 , similarly to form factors. Second, for the JLab data there is a nice agreement between the results obtained by the two methods, LET and DR. These new measurements should stimulate theoretical calculations of GPs at high Q^2 . Indeed most model predictions are presently limited to $Q^2 \ll 1 \text{ GeV}^2$.

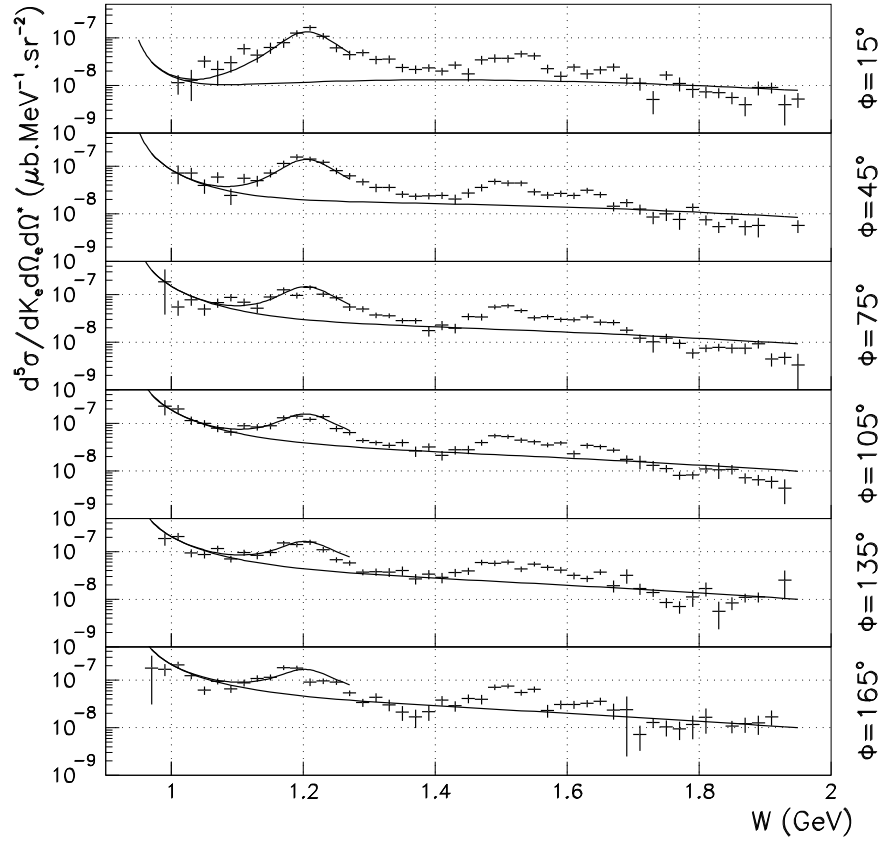


Figure 6: Photon electroproduction cross sections in the resonance region. The curve spanning the whole range in W is the BH+Born calculation. The curve limited to $W < 1.25$ GeV is the DR prediction for parameter values $\Lambda_\alpha = 1.0$ and $\Lambda_\beta = 0.45$ GeV.

3 Future prospects

Polarizabilities and Generalized Polarizabilities are intrinsic characteristics of composite particles. As such it is interesting to measure them for every hadron, including e.g. the neutron, pion, etc, although this may seem a task for the far future. Undoubtedly, investigations of the VCS process on the proton have been fruitful, and will continue to bring exciting new results in the coming years. Future developments are foreseen in various c.m. energy domains:

- at low energy, the mapping of the unpolarized structure functions ($P_{LL} - \frac{1}{\epsilon} P_{TT}$) and P_{LT} versus Q^2 can be completed, and P_{LL} and P_{TT} can be disentangled by an ϵ -separation. By studying $\vec{e}p \rightarrow e\vec{p}\gamma$ with a polarized beam and recoil proton

Table 3: Present results on VCS structure functions. ($\pm\bullet$) indicate that systematic errors are not fully determined. DR results at $Q^2 = 1.0 \text{ GeV}^2$ are from resonance region analysis.

Q^2 (GeV ²)	q (MeV/c)	ϵ	$P_{LL} - P_{TT}$ structure function (GeV ⁻²)		
0.33	600	0.62	LET: + 23.7	± 2.2 (stat)	± 4.3 (syst)
1.0	1080	0.95	LET: +2.32	± 0.22 (stat)	± 0.35 (syst) $\pm\bullet$
1.0	1133	0.95	DR : + 2.29	± 0.24 (stat)	$\begin{smallmatrix} -0.49 \\ +0.30 \end{smallmatrix}$ (syst)
1.9	1600	0.88	LET: + 0.56	± 0.07 (stat)	± 0.11 (syst) $\pm\bullet$
1.9	1600	0.88	DR : in [+0.43,+0.84]		
Q^2 (GeV ²)	q (MeV/c)	ϵ	P_{LT} structure function (GeV ⁻²)		
0.33	600	0.62	LET: - 5.0	± 0.8 (stat)	± 1.8 (syst)
1.0	1080	0.95	LET: - 0.42	± 0.11 (stat)	± 0.02 (syst) $\pm\bullet$
1.0	1133	0.95	DR : - 0.53	± 0.12 (stat)	$\begin{smallmatrix} -0.03 \\ +0.16 \end{smallmatrix}$ (syst)
1.9	1600	0.88	LET: +0.009	± 0.041 (stat)	± 0.005 (syst) $\pm\bullet$
1.9	1600	0.88	DR : in [-0.05,+0.02]		

polarimetry, one can in principle disentangle the six independent GPs entering the first order term of the LET, giving access to the spin GPs. Such experiments are planned at Mainz and Bates.

- In the resonance region, the VCS process was investigated for the first time by the JLab E93-050 experiment. It demonstrated the feasibility of GP extraction above pion threshold, owing to an enhanced sensitivity of the VCS cross section to GPs in the Delta resonance region. Future experiments along these lines at high Q^2 are foreseeable, either with or without polarization degrees of freedom.
- VCS at higher energies is certainly a very active field, with growing interest in Deep VCS and the GPDs. Using a longitudinally polarized electron beam, the HERMES and JLab-CLAS collaborations have determined a Single Spin Asymmetry in $\vec{e}p \rightarrow ep\gamma$ [18], giving the first input to GPD models, and more such experiments are planned at JLab, HERMES and COMPASS in the near future. As energies increase, experimental resolution limitations make it more and more difficult to isolate the one-photon electroproduction channel, and all present and future experiments plan to detect all three particles in the final state in order to reach exclusivity.

Acknowledgments

This work was supported by DOE, NSF, by contract DE-AC05-84ER40150 under which the Southeastern Universities Research Association (SURA) operates the

Thomas Jefferson National Accelerator Facility for DOE, by the French CEA, the UBP-Clermont-Fd and CNRS-IN2P3 (France), the FWO-Flanders and the BOF-Gent University (Belgium) and by the European Commission ERB FMRX-CT96-0008.

References

- [1] M. Diehl, these Proceedings.
- [2] M. Vanderhaeghen *et al.*, Nucl. Phys. A622 (1997) 144c.
- [3] V. Olmos de Leon *et al.*, Eur. Phys. J. A10 (2001) 207.
- [4] P. Guichon *et al.*, Nucl.Phys. A591 (1995) 606.
- [5] P. Guichon *et al.*, Prog. Part. Nucl. Phys. 41 (1998) 125.
- [6] B. Pasquini *et al.*, Eur. Phys. J. A11 (2001) 185, and these Proceedings.
- [7] J. Roche *et al.*, Phys. Rev. Lett. 85 (2000) 708.
- [8] T. Hemmert *et al.*, Phys. Rev. D55 (1997) 2630.
- [9] See ref. [8], [10], [6], and also: A. Metz *et al.*, Z. Phys. A356 (1996); G. Liu *et al.*, Aust. J. Phys. 49 (1996); B. Pasquini *et al.*, nucl-th/0105074.
- [10] M. Vanderhaeghen, Phys. Lett. B368 (1996) 13.
- [11] J. Shaw, R. Miskimen *et al.*, Bates Proposal E97-03 (1997).
- [12] N. Kaloskamis, C. Papanicolas *et al.*, Bates Proposal E97-05 (1997).
- [13] P. Bertin *et al.*, JLab proposal E93-050 (1993).
- [14] O. Gayou *et al.*, Phys. Rev. Lett. 88 (2002) 092301.
- [15] E. Brash *et al.*, Phys. Rev. C65 (2002) 051001.
- [16] G. Laveissière, Thesis DU 1309, UBP Clermont-Fd (2001), and also L. Todor, these Proceedings.
- [17] L. Van Hoorebeke, these Proceedings.
- [18] S. Stepanyan *et al.*, Phys. Rev. Lett. 87 (2001) 182002; A. Airapetian *et al.*, Phys. Rev. Lett. 87 (2001) 182001.